Syst. Biol. 0():1–13, 2020

DOI:10.1093/sysbio/syaa091

A Multifunction Trade-Off has Contrasting Effects on the Evolution of Form and Function

KATHERINE A. CORN*, CHRISTOPHER M. MARTINEZ, EDWARD D. BURRESS, AND PETER C. WAINWRIGHT

Department of Evolution & Ecology, University of California, Davis, 2320 Storer Hall, 1 Shields Ave, Davis, CA, 95616 USA
**Correspondence to be sent to: University of California, Davis, 2320 Storer Hall, 1 Shields Ave, Davis, CA 95618, USA; E-mail: kacorn@ucdavis.edu*

Received 27 August 2020; reviews returned 14 November 2020; accepted 19 November 2020
Associate Editor: Benoit Dayrat

Abstract.—Trade-offs caused by the use of an anatomical apparatus for more than one function are thought to be an important constraint on evolution. However, whether multifunctionality suppresses diversification of biomechanical systems is challenged by recent literature showing that traits more closely tied to trade-offs evolve more rapidly. We contrast the evolutionary dynamics of feeding mechanics and morphology between fishes that exclusively capture prey with suction and multifunctional species that augment this mechanism with biting behaviors to remove attached benthic prey. Diversification of feeding kinematic traits was, on average, over 13.5 times faster in suction feeders, consistent with constraint on biters due to mechanical trade-offs between biting and suction performance. Surprisingly, we found that the evolution of morphology contrasts directly with these differences in kinematic evolution, with significantly faster rates of evolution of head shape in biters. This system provides clear support for an often postulated, but rarely confirmed prediction that multifunctionality stifles functional diversification, while also illustrating the sometimes weak relationship between form and function. [Form-function evolution; geometric morphometrics; kinematic evolution; macroevolution; Ornstein–Uhlenbeck; RevBayes; suction feeding]

Morphological systems with more than one function may experience trade-offs tied to an inability to simultaneously optimize alternative functions (Futuyma and Moreno 1988; Wilson and Yoshimura 1994; Koehl 1997; Wainwright 2007). The compromises inherent in trade-offs suggest that multifunctionality discourages the incorporation of novel functions into existing repertoires, thereby limiting diversification of these systems (Schaefer and Lauder 1996; Gatesy and Middleton 1997; Bennett and Lenski 2007; Walker 2007; Farina et al. 2019). But, the efficacy of this suppressive effect has been called into question by recent research that finds that traits most closely tied to trade-offs show elevated rates of evolutionary diversification, demonstrating that trade-offs can sometimes promote rather than limit diversification (Holzman et al. 2012; Muñoz et al. 2017, 2018). These contrasting observations indicate a need for specific tests of multifunctional constraint, particularly as they suggest that the impact of a trade-off may be context-dependent. Furthermore, most studies of multifunctionality focus on underlying anatomical traits, but because the mapping of form to function can be complex, it is important to explore diversification at both levels (Koehl 1997). In this study, we asked how multifunctionality affects the evolution of the feeding mechanisms in fishes. We compared prey capture kinematics in fishes that feed with one mechanism, suction, with those of fishes potentially exposed to a trade-off invoked by having two prey capture mechanisms: suction and biting.

Suction feeding is used by nearly all aquatic vertebrates for prey capture. Highly versatile, suction is used to capture virtually any free-moving prey, including fishes, crustaceans, polychaetes, zooplankton, and insects (Lauder 1985). A suction strike involves rapid expansion of the skull that draws in water and prey, made possible by mobile cranial elements and by the high density and viscosity of water (Lauder 1980a; Sanford and Wainwright 2002; Westneat 2006). Across ray-finned fishes (Actinopterygii), for whom suction feeding is the ancestral mode of prey capture, skull expansion is achieved by way of flexible joints and many independently moving components (Schaeffer and Rosen 1961; Anker 1974; Elshoud-Oldenhave 1979; Lauder 1980a; Westneat 2006). Some fishes, especially in reef habitats, have expanded their feeding repertoire, using direct biting actions to remove attached prey not easily captured with suction (hereafter termed "biters") (Liem 1978, 1980; McKaye and Marsh 1983; Bellwood and Choat 1990; Konow and Bellwood 2005; Konow et al. 2008; Gibb et al. 2015). Biters continue to use suction, but habitual biting or grazing places novel functional requirements on their cranial anatomy (Bemis and Lauder 1986; Gillis and Lauder 1995; Van Wassenbergh et al. 2007; Ferry et al. 2012; Mackey et al. 2014). A biting strike typically transmits greater forces through the jaws to the prey or substrate than a suction strike (Liem 1979; McGee et al. 2016). Elevated forces in biters are expected to lead to greater cranial strength and stability, but a reduction in mobility as a result of a fundamental trade-off between transmitting motion versus force through the musculoskeletal levers that form the kinetic fish skull (Kotrschal 1988; Westneat 1994; Ferry-Graham and Konow 2010; McGee et al. 2016; Martinez et al. 2018).

We explored the impact of multifunctionality associated with biting on diversification of the feeding mechanism by comparing the rates of evolution of cranial mobility measured during prey capture in 44 species of suction feeders and biters spanning 28 families of fishes of percomorph fishes (Percomorpha includes about 160 families). Using landmark morphometrics applied to high-speed videos of fishes feeding, we generated a data set consisting of seven traits capturing cranial motions during suction feeding.

We then estimated rates of evolution, trait optima, and convergence of suction kinematics, as well as the evolutionary rate of cranial morphology. We used two contrasting approaches to assess evolutionary rates of cranial mobility (e.g., kinesis) and major components of kinesis (e.g., jaw protrusion, rotation, gape, etc.), one based on a univariate Brownian Motion and Ornstein–Uhlenbeck model-fitting framework, and a second with a Bayesian, relaxed clock, state-dependent, multivariate model of Brownian Motion. If a trade-off between mobility and force transmission constrains the evolution of prey capture kinematics, we should see slower rates of evolution in species that use both biting and suction, versus those using suction alone.

Materials and Methods

Data Set Construction

Feeding mode distribution.— We categorized species in our study as either "biting," referencing those species that use both biting and suction, or "suction feeding" based on published information about their feeding ecology and our own observations in the lab and the field (Purcell and Bellwood 1993; Westneat 1995; Randall et al. 1997; Ferry-Graham et al. 2001; Wainwright and Bellwood 2002; Konow et al. 2008; Oufiero et al. 2012; Copus and Gibb 2013). We classified a "biting" feeding mode as one where the fish uses suction as well as direct biting actions. A direct biting action was designated as one where the fish's closing jaws make contact with the prey item to either grip it or scrape it from a holdfast. We identified 31 suction feeders and 13 biters in our data set of 44 species (Supplementary Table S1 available on Dryad at https://doi.org/10.25338/B8703S).

Feeding videos and landmark morphometrics.—We collected 175 lateral view high-speed videos of suction-based feeding strikes in 44 species of fishes from 28 families within Percomorpha for which we had identified feeding mode. To calculate overall cranial kinesis, we used the method described by Martinez et al. (2018), summarized here. Landmark morphometrics was used to digitally capture head shape at 10 equidistant time points during each feeding strike, starting with the onset of mouth opening and ending when maximum gape was achieved. We used tpsDig2 (Rohlf 2015) to place 18 landmarks on the fish's head: 10 fixed landmarks denoted functionally informed, homologous points of the cranial anatomy and eight sliding semilandmarks along the ventral margin of the head captured the motion of the lower jaw and depression of the hyoid apparatus of the throat, which

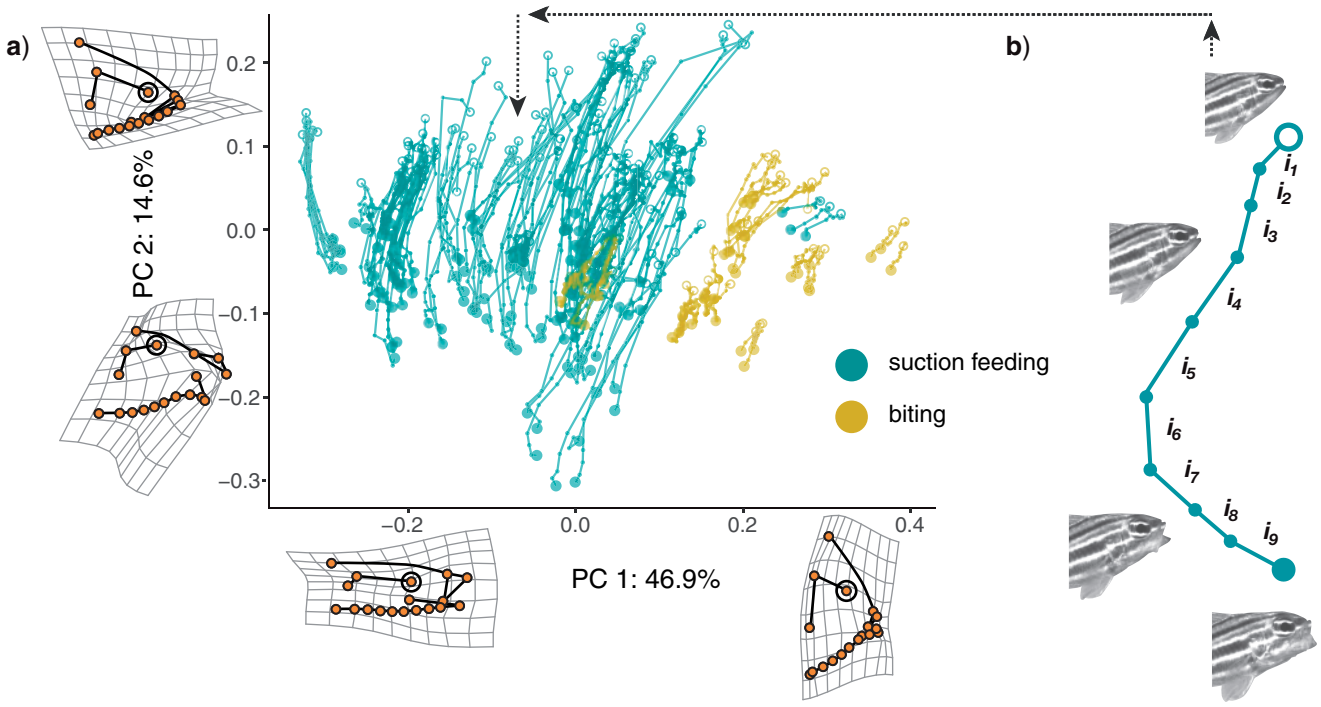

FIGURE 1. Comparison of motion trajectories of suction-feeding strikes by fishes that naturally feed with either a biting or suction-based feeding mode. a) 175 feeding sequence motion trajectories displayed on PCs 1 and 2, colored by feeding mode. Individual lines connect frames that are part of a single feeding sequence, and each point along the lines reflects head shape during one of the 10 sampled frames of the video sequence. Larger points at the ends of lines indicate starting postures (i.e., closed mouth, shown as an open point) and maximum gape (closed point), and smaller points represent intermediate motion points. All strikes proceed in a generally downward direction on the plot. Deformation grids indicate landmark positions at minima and maxima for each PC; the position of the eye is circled. The major axis of variation corresponded with head shape diversity (PC1), followed by an axis of shape change largely associated with feeding motions (PC2). b) Mock illustration in the style of sequences shown in a, displaying shape change of a fish head during a single suction feeding event and the resulting shape trajectory.

we refer to as "buccal depression" (Supplementary Fig. S1 available on Dryad). Landmark data were analyzed in the statistical software R v. 3.6.3 (R Core Team 2019) using the package *geomorph* v. 3.1.2 (Adams and Otárola-Castillo 2013). A generalized Procrustes analysis (GPA) was performed to align the data, an iterative process of scaling, rotating, and translating all shapes to reduce the Procrustes distance between them (Rohlf and Slice 1990). Alignment of sliding semilandmarks during GPA was done in a manner that reduced Procrustes distance (Gunz and Mitteroecker 2013). We extracted head shape data from the starting image of each strike, when the mouth was closed, computed a separate alignment for those shapes, and then averaged them by specimen and then by species. This procedure for extracting head shape data from video sequences resulted in a morphological data set in which all downstream analyses of head shape were independent of scale.

Calculating total cranial kinesis and kinematic components.—We visualized each feeding strike as a trajectory of head shape change. The length of this trajectory was quantified using Procrustes distance, which represents the distance between two points (i.e., shapes) in shape space (Kendall 1984; Adams and Otárola-Castillo 2013) (distances i_j in Fig. 1b). This resulted in nine distances between the 10 head shapes representing a strike sequence, which we summed to get the total trajectory length, representing overall cranial kinesis (sum of i_1:i_9 in Fig. 1b). A longer shape change trajectory represented higher kinesis, with a greater range of motion of cranial bones (Martinez et al. 2018; Martinez and Wainwright 2019). We separately measured six components of cranial kinesis from the landmark data, which we refer to as "kinematic components" (Supplementary Fig. S2 available on Dryad). These measurements included the peak values of major elements of the expansive phase of a suction strike: upper jaw protrusion, mouth gape, cranial elevation, upper jaw rotation, lower jaw rotation, and buccal depression (Supplementary Fig. S2 available on Dryad). These kinematic components are functionally integrated into a suction feeding strike and their sequential, coordinated activation is a defining feature of suction feeding (Gibb and Ferry-Graham 2005; Bishop et al. 2008; Olsen et al. 2019). All measurements, including overall cranial kinesis and all six kinematic components, were computed for each feeding strike and averaged at the specimen-, then species-levels prior to conducting statistical analyses.

Data Analysis

Phylogenetic comparative methods.—To account for the effects of shared evolutionary history on kinematic and morphological traits, we employed a dual model-fitting approach to estimate the impact of native feeding mode (suction or biting) on the rate of evolutionary diversification of kinematics during suction-based feeding events. We pruned a large phylogeny of ray-finned fishes (Rabosky et al. 2018) to the species in our data set and used the R packages *stats*, *ape* v 5.3 (Paradis et al. 2004), and *phytools* 0.6-99 (Revell 2012) to explore evolutionary patterns. Where species in our data set were not present in the phylogeny, we substituted them with a species chosen at random from those in the same genus or the most closely related genus that were sampled in the tree; four species required this substitution (genera: within-*Choerodon*; *Oxycirrhites* to *Paracirrhites*; *Cyprinocirrhites* to *Notocirrhitus*; *Terelabrus* to *Bodianus*).

We estimated disparity separately for each kinematic trait using morphol.disparity in *geomorph*, and also took the average of all seven values. Separate phylogenetic ANOVAs using procD.pgls in *geomorph* were used to compare overall cranial kinesis and individual kinematic components by feeding mode (at $\alpha = 0.05$). We used principal component analysis (PCA) on the correlation matrix to visualize the multivariate kinematic data. Lastly, to compare head morphology, we visualized the morphospace of interspecific head shape variation from landmark data using the plotTangentSpace function in *geomorph* and measured overall morphological disparity with the morphol.disparity function in that R package.

Convergent evolution.—We used two distance-based metrics of evolutionary convergence, as implemented in the package *convevol* v 1.3 (Stayton 2015). We estimated convergent evolution among biting lineages in our kinematic data, including overall cranial kinesis and the six kinematic components. C_1 estimates the proportion of phenotypic distance closed by the evolution of the putatively convergent tips, given the maximum distance in phenotypic space between lineages, including estimated ancestral states at nodes (Stayton 2015). We also compared C_3, which estimates the proportion of the total evolution of the putatively convergent taxa distance that brings taxa closer together, or that which is "attributable to convergence." We ran significance tests using 500 simulations of convratsig when estimating the degree of convergence in kinematic data, which iterates the distance-based convergence tests.

Evolutionary rate and trait optima estimates.—There are no reliable methods yet to model the effect of a discrete trait in a multivariate Ornstein–Uhlenbeck framework for very high-dimensional data, like the morphometric landmarks that we used to capture head shape (Adams and Collyer 2018, 2019). Therefore, we used multivariate Brownian Motion models implemented in *geomorph* to estimate the evolutionary rates and compared the fit of single- and multirate Brownian motion models (Adams and Otárola-Castillo 2013; Adams 2014). We used feeding mode as a binary discrete trait.

We used a 2-fold methodology to estimate rates of character evolution for kinematic components and kinesis for biters and suction feeders. In the first

approach, we fit a series of Brownian Motion (BM) and Ornstein–Uhlenbeck (OU) models of trait evolution to estimate univariate evolutionary rates. Both BM and OU models can be used to estimate evolutionary rate of a continuous character and to test for the effect of discrete trait history on continuous character evolution. We used feeding mode as a binary discrete character and generated a distribution of 1000 stochastic character maps using *phytools* (Revell 2012). For kinesis and each kinematic component, we then fit five BM or OU models on each stochastic character map using *OUwie* (Beaulieu et al. 2012). We fit single-rate Brownian Motion, "BM1"; multirate Brownian Motion, "BMS"; single rate, single optimum Ornstein–Uhlenbeck, "OU1"; multioptimum, single-rate Ornstein–Uhlenbeck, "OUM", and multirate, multipeak Ornstein–Uhlenbeck, "OUMV". We elected not to fit multirate, multipeak, multiselection Ornstein–Uhlenbeck models with a separately estimated sigma-squared and alpha (OUMVA) because of difficulties with interpreting values of sigma-squared under different estimates of the alpha parameter (Ho and Ané 2014; Cooper et al. 2016). We compared the fit of models across all 1000 stochastic character maps using AICc, with a distinguishability cutoff of 2.0.

Secondly, we fit estimated rates of kinematic evolution in suction feeders and biters with a Bayesian approach, using a relaxed clock, state-dependent, multivariate BM model of evolution, implemented with the MuSSCRat model and executed in RevBayes (Höhna et al. 2016; May and Moore 2019). We used the MuSSCRat model for estimates of evolutionary rate because it allows multivariate estimates of the Brownian rate parameter, jointly estimates evolution of the discrete trait and the continuous traits avoiding a source of bias in rate estimates (Revell 2013) and uses a relaxed-clock model incorporating background rate variation that provides improved type-I error rates (May and Moore 2019). Most common implementations of BM or OU are univariate, allowing only one continuous character at a time (Adams 2014; Denton and Adams 2015; Adams and Collyer 2018, 2019). However, the multiple kinematic components measured in our fishes are mechanically linked and are concurrently activated during a feeding strike. For this reason, a multivariate approach that allows us to capture that covariation is valuable. Furthermore, a state-dependent, relaxed-clock model allowed us to directly test our hypothesis that the rate of evolution depends on feeding mode, at the exclusion of other sources of rate variation.

We ran three separate MCMCs of the MuSSCRat model due to unit incommensurability between the three forms of measurement data (Huttegger and Mitteroecker 2011; Adams and Collyer 2019). We fit independent models with the three angular kinematic components, the three linear distance components, and overall cranial kinesis as continuous characters and used feeding mode

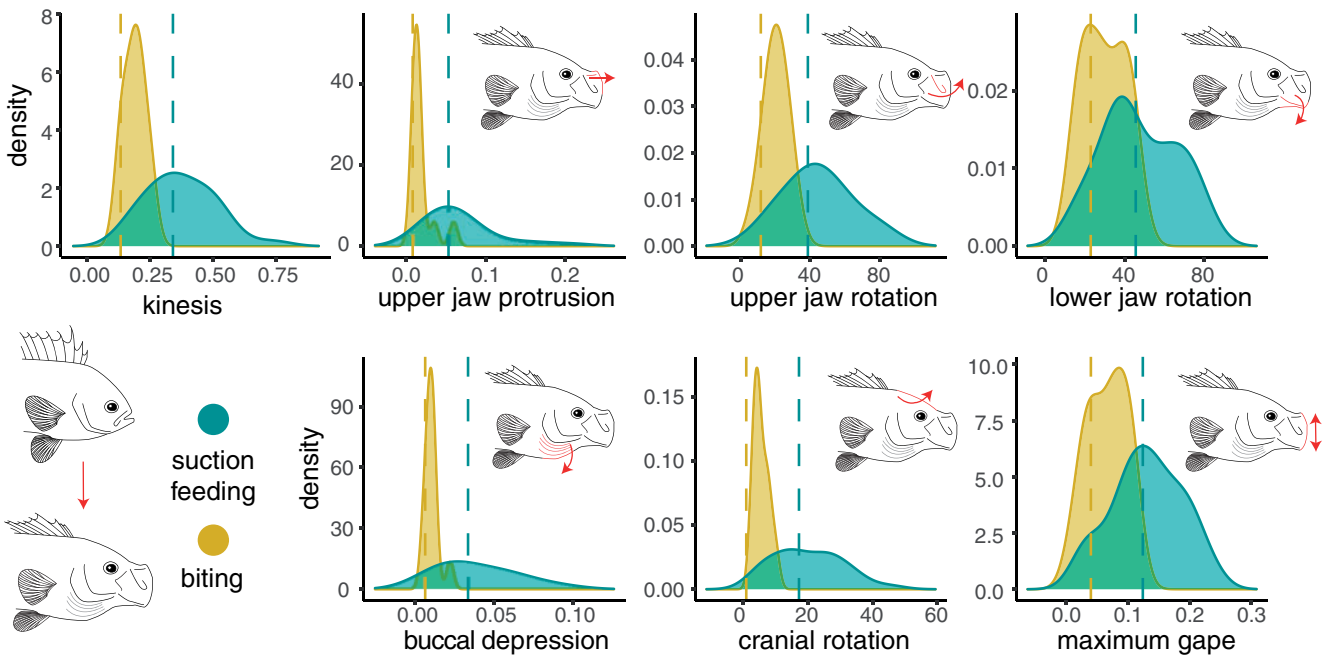

FIGURE 2. Major kinematic components in fishes that use suction and biting feeding modes and their evolutionary optima. Density plots depict the maximum value of each measured variable attained during a feeding sequence, averaged by species. Dashed lines indicate the evolutionary optima (theta) estimated by the multi-rate, multi-optima Ornstein–Uhlenbeck model (OUMV), colored by feeding group. Phylogenetic ANOVAs for all kinematic traits were significant at $\alpha = 0.05$, except for lower jaw rotation. In every measured kinematic component and in overall kinesis, biters have both lower values and lower variance among-species, relative to suction feeders. Illustrated on the left are starting and maximum gape postures of *Paranthias furcifer*; illustrated at each panel is the motion measured by that kinematic component. Arrows show the direction of motion, with mobile anatomy that has been measured marked in the same color.

(biting and suction feeding) as a binary discrete trait. The MCMCs ran for 500,000 generations (distances), 1 million generations (angles), or 2 million generations (kinesis) with a 10% burn-in, and we set a prior expectation on the number of transitions between discrete states at 5 for all models. We drew transition rates from a log-normal prior and set a log-uniform prior on the probability that the rate of the continuous characters was state-dependent. A log-normal prior informed the rate shift distribution. We describe how we evaluated the influence of priors on the number of rate shifts on posterior parameter estimates in the Supplementary Methods available on Dryad (Supplementary Fig. S5 available on Dryad).

Results

Diversity in kinematics and morphology

Overall cranial kinesis and kinematic components.—Suction feeding fishes had greater overall cranial kinesis, undergoing greater total shape change during feeding strikes, than did biters (Fig. 1). Across six components of cranial mobility, suction feeders had more diverse feeding kinematics, possessing an average of 13.53-fold greater variance among species than in biters (Supplementary Table S2 available on Dryad). Additionally, fishes that use biting had smaller mean values than those that use only suction for all kinematic components except for lower jaw rotation and also displayed lower overall cranial kinesis (Fig. 2; Supplementary Table S3 available on Dryad). A PCA of the six kinematic components resulted in all variables loading positively on PC1, which accounted for 65.9% of total variation and represented an axis of low to high mobility, with biters clustered low on PC1. PC2 (17.8% of total variation) primarily captured variation among suction feeders, with upper jaw protrusion and maxillary rotation loading positively and highly, but maximum gape loading strongly, but negatively on this axis (Fig. 3a; Supplementary Fig. S3 and Table S4 available on Dryad).

Head shape diversity.—Feeding mode had a strong effect on head shape. When visualized in the first two axes of a PCA, feeding mode separated species into two minimally overlapping groups (Fig. 3b). Head depth and mouth size were major contributors to this separation, correlating most strongly with PC1 (40% of total variation) and PC2, respectively (29.1% of total variation). Biters occupied parts of the morphospace associated with deeper heads and smaller mouths as compared to suction feeders. Disparity (i.e., variance) of head shape in suction feeders was 1.54× that of biters but was not statistically different ($p = 0.15$).

Convergence among biters.—We found strong evidence for convergent evolution in the kinematics of species that use both biting and suction ($C_1 = 0.404$; $P < 0.0001$), indicating that biters have closed 40% of the maximum distance in kinematic phenotype space between their lineages. An estimated 20.2% of the total evolution of kinematic components and total cranial kinesis in biters brought these putatively convergent taxa closer together (C_3) (Fig. 4). Consistent with the results for trait means and variances, biters converged on lower cranial kinesis and lower variation among species in kinesis than suction feeding species.

Models of Evolution

Stochastic character maps.—A distribution of 1000 stochastic character maps, simulating the discrete character history of feeding mode, recovered an average of 9.00 transitions between states, including some from suction to biting, and others back again from biting to suction (Fig. 5a). Reconstructions predict the ancestral character state of the sampled taxa to be suction feeding.

Morphological evolution.—Head shape evolved faster in biters than in suction feeders, with the former having about a 1.62-fold faster rate of evolution. Model fitting significantly favored different rates for feeding mode groups over a single-rate model (BMS preferred over BM1, $P = 0.01$). Though biters have an elevated rate of head shape evolution compared to suction feeders, their slightly lower disparity is likely due to the smaller proportion of time on the phylogeny spent in a biting state.

Kinematic evolution.— In a Brownian Motion and Ornstein–Uhlenbeck model-fitting framework, suction feeders had elevated rates of evolution when compared to biters in all six kinematic components as well as total cranial kinesis (Fig. 5b, Table 1). All traits were best fit by a multirate, multioptima model of evolution (OUMV), but some traits were equally well fit by either multirate Brownian Motion with no adaptive optima (BMS; buccal depression, head rotation) or a single-rate, multioptima model (OUM; lower jaw rotation, maximum gape). As all traits were equally well or best fit by the OUMV model, we reference its parameters for the rest of this manuscript, particularly when comparing this model-fitting framework to an alternative approach used, below. Suction feeders always had an optimum associated with larger trait values than biters (Fig. 2). Furthermore, in suction feeders, model-predicted trait optima were largely aligned with the central peaks of empirically measured trait values, but observed trait distributions in biters were often centered on a peak associated with slightly higher trait values than those predicted by the model. Rates of evolution for kinematic traits were, on average, 16.53 times faster in suction feeders than biters, with the difference ranging from a 2.99-fold faster rate in a maximum gape to an exceptional 47.40-fold faster rate of upper jaw protrusion in suction feeders.

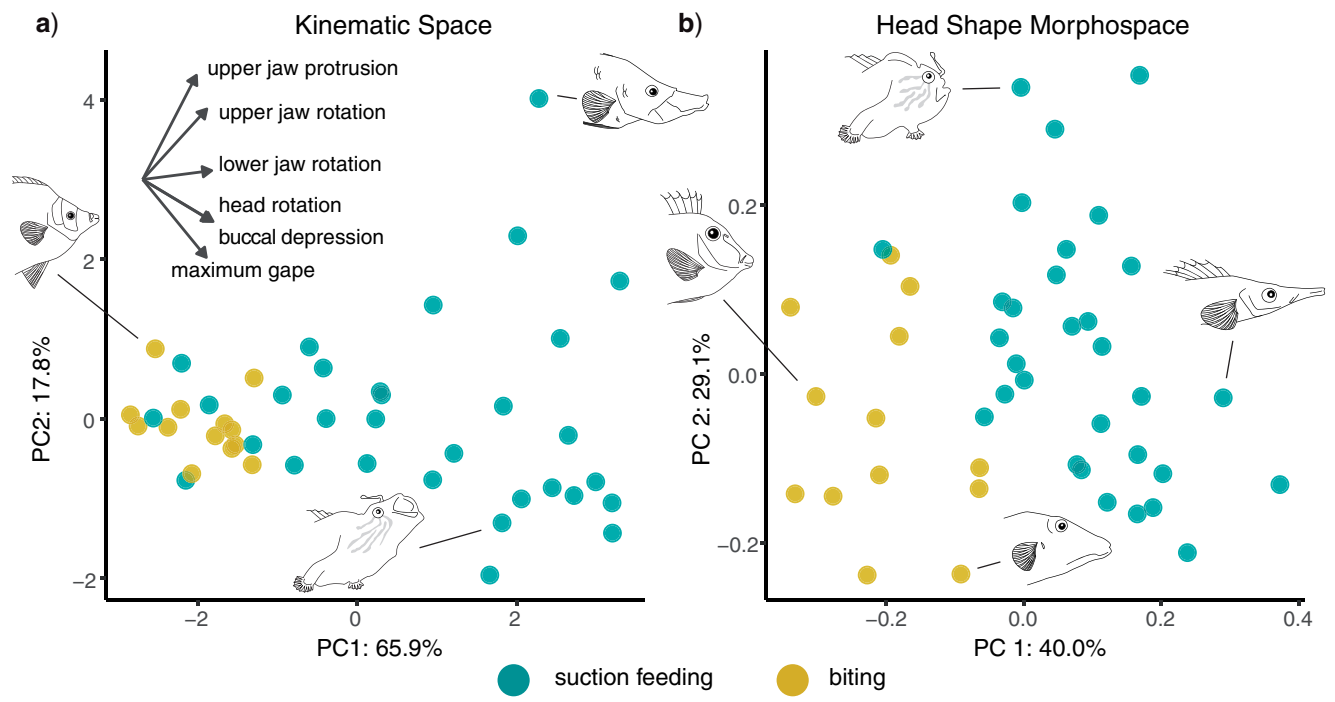

FIGURE 3. Distribution of biting and suction feeding fishes in kinematic and morphological space. a) Principal component axes (PCs) 1 and 2 from a PCA of six kinematic components. Points represent species' means. Note that suction feeders occupy much larger ranges than biters on PCs 1 and 2. Vectors in upper left inset represent PC loadings of kinematic components. Illustrated species at maximum gape posture, clockwise, starting from left: *Chaetodon lunula*; *Epibulus insidiator*; *Antennarius hispidus*. b) Morphospace of head shapes based on landmark morphometric data. Within the space defined by PCs 1 and 2, the two feeding modes have minimal overlap in shape. Illustrated head shapes (closed mouth posture) of selected species, clockwise, starting from left: *Naso elegans*; *Antennarius hispidus*; *Oxycirrhites typus*; *Canthigaster bennetti*.

An alternate method for rate estimation, using Bayesian relaxed-clock, multivariate, state-dependent models of evolution, reported an average of 13.50-fold faster evolution of kinematics in suction feeders than in biters while accounting for background rate variation, across three models (Fig. 6). Suction feeders evolved kinesis 15.13 times faster than biters, with a posterior probability of separate rates for each discrete state of 0.997 and an estimated 5.29 rate shifts. For linear distance-based components, suction feeders evolved 22.46-fold faster than biters, with a posterior probability of 1.00 for state dependence of the rate and an estimated 8.34 rate shifts. For angle-based components, suction feeders evolved 2.91 times faster than biters, with a posterior probability of state dependence of 0.91 and an estimated 7.13 rate shifts. The magnitude of the effect of feeding mode on trait evolution was variable; in kinesis, there was a strikingly strong correspondence between variation in rates that was attributed to the discrete trait and the overall rates for each branch (Fig. 6, Supplementary Fig. S4 available on Dryad). In contrast, the distance component traits and angle component traits showed a more moderate role for background rate variation contributing to overall branch rates.

DISCUSSION

We found patterns of diversity in fish feeding motions that are consistent with a trade-off constraining evolution in species with multifunctional jaws used for both biting and suction, compared to species that feed only by suction. Our results show a dominant role of multifunctionality in governing the evolution of suction strikes and of cranial mobility, with exceptional rate differences between groups: 16.5-fold per-trait average or a still high 13.5-fold (multivariate BM rate) faster evolution of species that use just suction feeding, even when accounting for background rate evolution. This very strong effect of feeding mode is underscored by the remarkable similarity in the evolution of total cranial kinesis between overall branch rates of evolution (Fig. 6a, center) and rate attributed to feeding mode, indicating that feeding mode accounts for nearly the full range of rates of evolution of suction feeding kinematics (Fig. 6a, right). We found that the constraints of the trade-off have limited both the degree of kinesis as well as the diversity of kinematic combinations in species that use both biting and suction when they feed using suction. In contrast, suction feeders have elevated kinematic diversity in part because of the higher degree of cranial

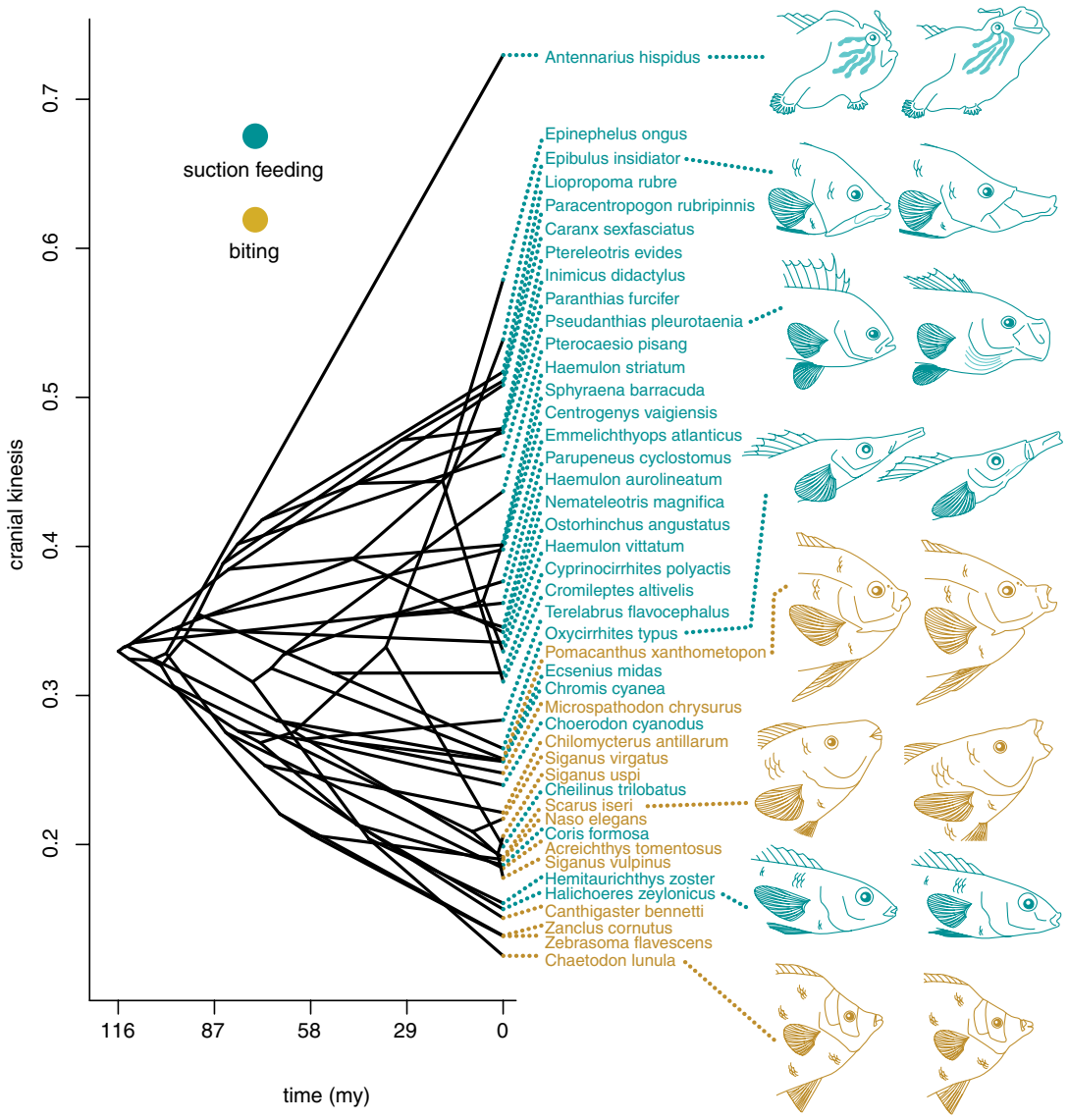

FIGURE 4. The evolutionary history of overall cranial kinesis among fishes. The y-axis is total cranial kinesis measured during suction-feeding strikes. Selected species have been drawn in starting and maximum gape postures to illustrate the range of overall cranial kinesis found in our data set. Illustrated fishes, as well as species names, have been colored by feeding mode. Internal branches and nodes were estimated using maximum-likelihood with the phenogram function in *phytools* (Revell 2012).

kinesis, but also because they couple their highly mobile strikes with varied contributions from different kinematic components to the overall feeding motion (Fig. 3a). For example, two of the highest kinesis suction feeders, *Antennarius hispidus* and *Epibulus insidiator*, have either high buccal expansion and comparatively modest jaw protrusion, or exceptional jaw protrusion with little buccal expansion, respectively.

Reduced kinesis appears to be adaptive for biting fishes with a multifunctional feeding apparatus, with lower rates of kinematic evolution across multiple model-fitting methods. Because of the inherent mechanical trade-off in levers between transmission of force and motion (Westneat 1994, 2003), adaptation in a feeding system that uses biting toward the transmission and application of force during biting results in less mobility during suction strikes. In a biting strike, the force applied to the prey item is transmitted directly through the jaw lever systems, which may lead to the evolution of efficient muscular force transmission and constraint of skeletal movement to minimize misalignment of force and motion (Tedman 1980; Kotrschal 1988; Bellwood and Choat 1990; Vial and Ojeda 1990; Friel and Wainwright 1997; Wainwright and Bellwood 2002; Ferry-Graham and Konow 2010; McGee et al. 2016). These expectations for the design of

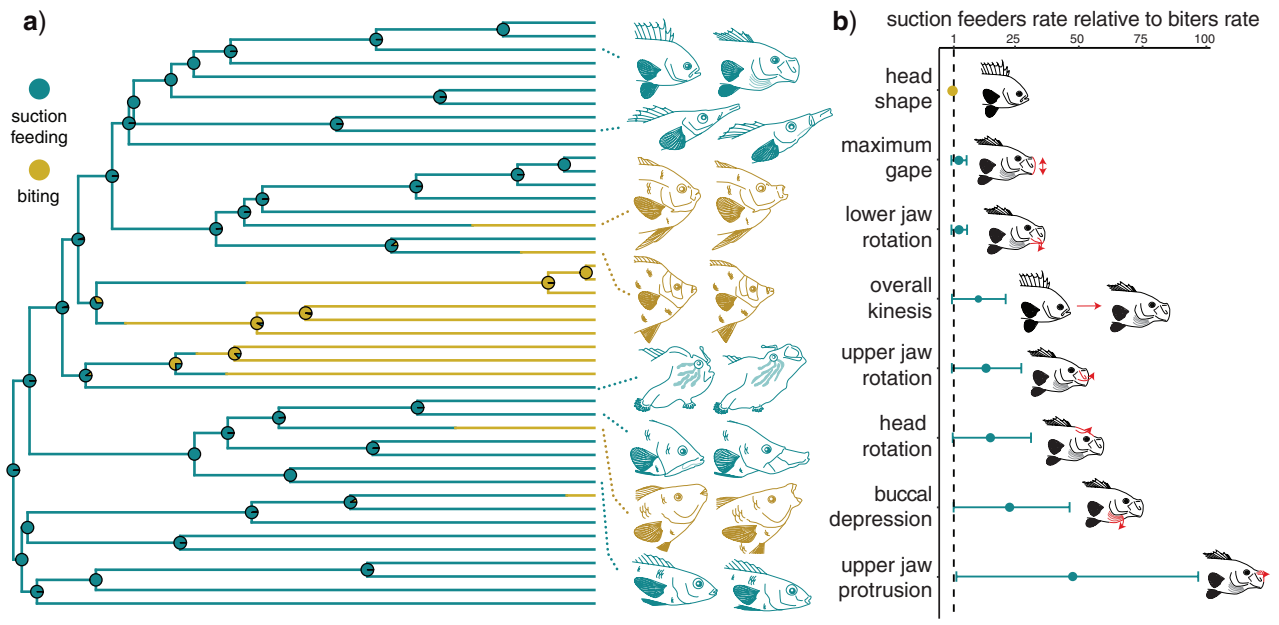

FIGURE 5. Results of macroevolutionary models in a Brownian Motion and Ornstein–Uhlenbeck model-fitting framework. a) Sample stochastic character map of feeding mode history, with pie charts at each node indicating the frequencies of each state, across 1,000 stochastic character maps. Select taxa have been drawn in their closed mouth and maximum gape postures to the right. b) Rate ratios of suction feeding species to biting species for multi-rate, multi-optima Ornstein–Uhlenbeck (OUMV) models for each trait except head shape, where multi-rate Brownian Motion (BMS) estimated the rate. Bars indicate 95% confidence intervals. Coloration indicates which group (biting or suction) had a higher rate. The dashed line, at 1, marks where the rates of evolution of suction feeders and biters are equal.

TABLE 1. Best-fitting evolutionary models from Ornstein–Uhlenbeck model fitting.

Trait	Model	AICc	AICc diff.	% best model	σ^2 ratio	Alpha	Θ_{biters}	$\Theta_{suction}$
Maximum gape	OUM	−131.59	0.62	93.3	1.00	0.01	0.03	0.13
	OUMV	−131.87	0.34	97.7	2.99	0.02	0.04	0.12
Head rotation	BMS	316.95	1.78	74.9	6.46	—	—	—
	OUMV	315.37	0.23	96.2	15.35	0.03	1.06	17.31
Buccal depression	BMS	−224.53	0.04	99.5	20.15	—	—	—
	OUMV	−223.31	1.28	95.0	22.73	0.01	0.01	0.03
Kinesis	OUMV	−63.03	0.07	95.8	10.52	0.05	0.13	0.34
Lower jaw rotation	OUM	380.56	1.05	80.8	1.00	0.02	19.34	46.00
	OUMV	379.93	0.50	85.4	3.07	0.06	22.87	45.61
Upper jaw rotation	OUMV	372.25	0.01	99.4	13.62	0.02	11.38	38.54
Upper jaw protrusion	OUMV	−172.82	0.01	97.0	47.40	0.13	0.01	0.05

Notes: We fit single-rate Brownian Motion, "BM1"; multi-rate Brownian Motion, "BMS"; single rate, single optimum Ornstein–Uhlenbeck, "OU1"; multi-optimum, single rate Ornstein–Uhlenbeck, "OUM", and multi-rate, multi-peak Ornstein–Uhlenbeck, "OUMV". We display multiple models in the cases where more than one model was considered 'equally likely' by AICc. The sum of "total percent best model" for a single trait may exceed 100% in cases where more than one model was consistently identified as best- or equally well-fitting. "σ^2 ratio" is the ratio of σ^2 estimated in suction feeders relative to biters, under the best fitting model.

a biting feeding system contrast with characteristics of suction strikes, which often include a large expansion of the buccal cavity to drive the flow of water into the mouth (Elshoud-Oldenhave 1979; Lauder 1980b; Camp et al. 2015; Jacobs and Holzman 2018), including jaw protrusion that increases the hydrodynamic forces that suction feeders exert on prey (Holzman et al. 2008; Staab et al. 2012).

Many biting taxa in our study have lost independent mobility between the two major bones of the upper jaw (Gosline 1987; Kotrschal 1988 and Bellwood 1993). Loss of independent upper jaw mobility results in less complex motion of the bones and, in most cases, the loss of upper jaw protrusion altogether, likely contributing to the extreme difference between groups in evolutionary rates for this trait (47.4-fold faster in suction feeders). The relationship between loss of mobility and reduced diversity of kinematics is reminiscent of the pattern in terrestrial vertebrate locomotion where an increased number of mobile elements is associated with

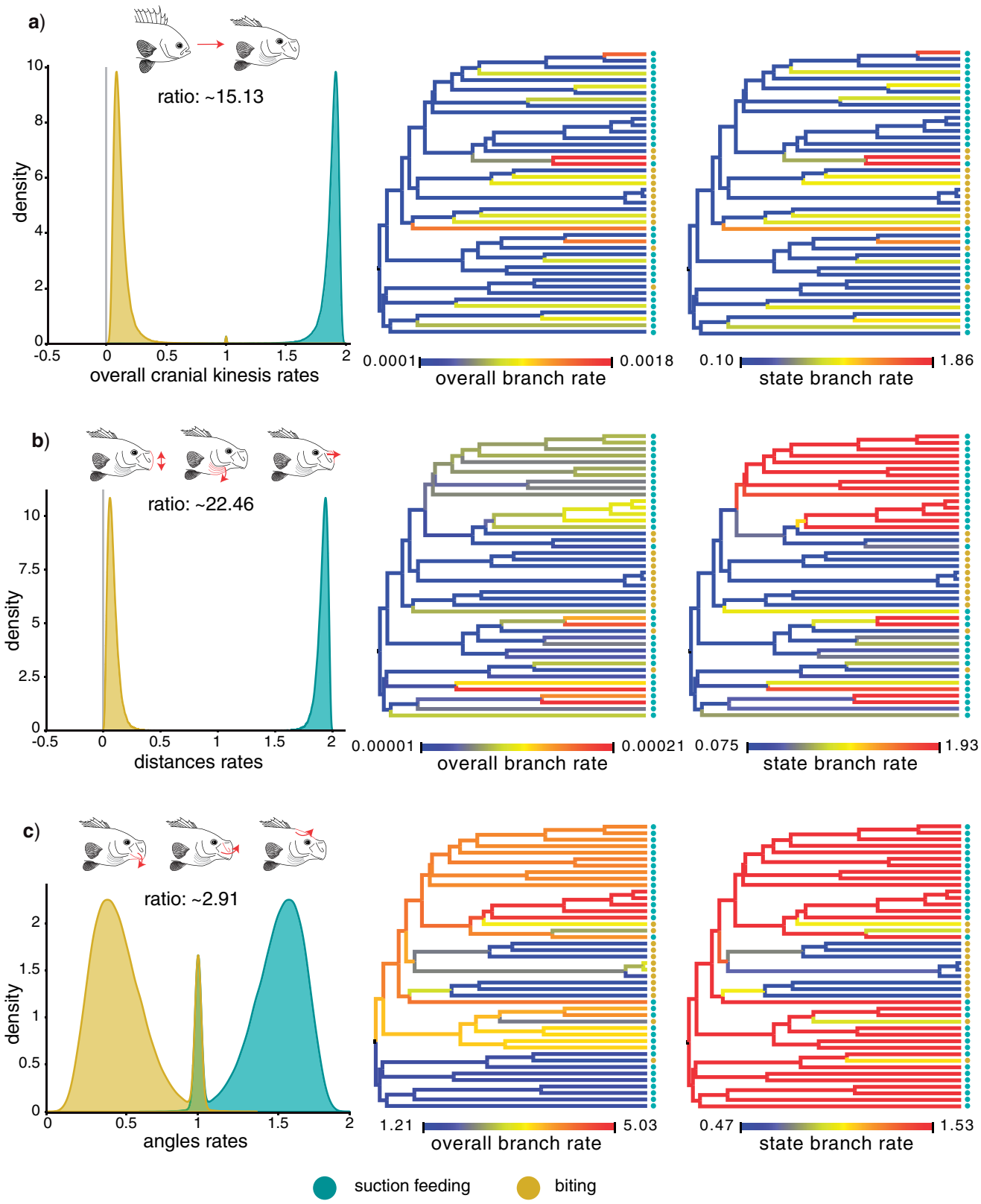

FIGURE 6. Results of macroevolutionary model-fitting with a Bayesian, multivariate, state-dependent, relaxed clock model of Brownian Motion across 3 models, showing substantial support for independent rates for each feeding mode state. Left, the posterior density distributions of the rates for each group colored by feeding mode. Center, overall per-branch rate estimates are mapped onto the phylogeny. Right, rate variation that is attributed to the discrete state are mapped onto the phylogeny. Center and right, on branches warmer colors indicate higher rates and cooler colors, lower rates. To the right of tree tips, circles indicate the feeding mode state for each species. a) Model-fitting on overall cranial kinesis showed strong support for distinct rates between groups, with most of the rate variation explained by the feeding mode state. b) The three distance-based traits showed strong support for distinct rates between groups but a more moderate effect of background rate evolution, seen in the increased disparity between the overall rates and the rate variation attributed to the discrete trait. c) The three angle-based traits, while still strongly supporting two discrete rate classes, show a peak indicating a lower probability of identical rates between groups. Notably, the relationship between branch rate and feeding mode state is very pronounced in angle state-dependent rates, as suction feeders uniformly have higher rate than biters.

diversity in locomotor patterns (Mosauer 1932; Dagg 1973; Hildebrand 1989). For example, mammals that almost exclusively move their hind legs synchronously, like adult rabbits, have fewer gaits than animals that routinely move each of their four limbs in different patterns (e.g., horses). Such a relationship between diversification and number of independent elements is consistent with the literature on modularity, which suggests that an elevated number of modules may increase the evolvability of the system, or its ability to vary (Hallgrímsson et al. 2009). Interestingly, the observed distribution of biters for each kinematic trait is centered around a slightly larger value than the optima estimated by Ornstein–Uhlenbeck models (Fig. 2), possibly reflecting compromises required to maintain adequate mobility to produce effective suction or that these species have yet to reach the optimal trait values. We conclude that convergent evolution of reduced cranial mobility during suction feeding may be a consequence of trade-offs that are characteristic of a multifunctional feeding apparatus, providing an example of how specialization for one function may have major consequences for another, within the context of a multifunctional apparatus.

Much of the observed diversity among suction feeders appears to be associated with the different prey that these species normally feed on. Our sample includes piscivores with a large mouth opening and substantial buccal expansion (e.g., *Antennarius hispidus, Epinephelus ongus*), predators of small fish and elusive invertebrates with a high degree of upper jaw rotation (e.g., *Epibulus insidiator, Oxycirrhites typus*), and species that crush shelled prey in the pharyngeal jaws but capture them with suction (e.g., *Cheilinus trilobatus*) (Hiatt and Strasburg 1960; Grobecker and Pietsch 1979; Ormond 1980; Cornic 1987; Myers 1991; Wainwright and Richard 1995; Randall et al. 1997; Craig 2007). The higher rate of kinematic evolution in native suction feeders suggests that changes to the kinematic pattern, achieved by varying the amount and relative contribution of different skull motions, are a key part of the adaptive diversification of this feeding behavior, an insight that is supported by literature pointing to trends between feeding kinematics and trophic ecology (Liem 1978, 1979, 1980; Norton and Brainerd 1993; Norton 1995; Rupp and Hulsey 2014; Longo et al. 2016; Martinez et al. 2018).

Surprisingly, the observed difference in the rate of evolution of feeding kinematics is not associated with a parallel pattern in cranial morphology, as we found that relative to biters, suction feeders have an average of at least 13.50-fold faster kinematic evolution, but biters have 1.62-fold faster rates of evolution of head shape (Fig. 5b). It is possible that the substantial kinematic constraints imposed by a biting feeding mode have spurred the evolution of the cranial morphology to meet those requirements. While a more detailed exploration of morphology may reveal greater anatomical diversity in specific structures in suction feeders, this result indicates that kinematic evolution reflects something more than a simple mapping of function onto morphology (Koehl 1997; Wainwright 2007). By extension, the impressive morphological diversity of suction feeding ray-finned fishes may substantially underestimate their kinematic diversity, whereas fishes that rely on biting have less kinematic diversity than would be expected from their morphological variation. This result also suggests that caution is warranted when inferring functional traits from morphology, a key step in many ecomorphological studies (Feilich and López-Fernández 2019).

Our study demonstrates that the effects of multifunctional trade-offs are not restricted to phenotype or functional space occupation, but also affect evolutionary rates in the involved traits and functions. The role of trade-offs in determining the occupation of morphospace has been documented in some taxa. In turtles, interactions of hydrodynamics, self-righting ability, and mechanical stiffness constrain shell shape, and the trade-offs between these functions can pull species between optima (Polly et al. 2016; Stayton 2019; Polly 2020); in birds, the release of trade-offs on the hindlimbs as the forelimbs evolve to be used for flight results in elevated diversity of the hindlimb (Gatesy and Middleton 1997); and in land plants, an adaptive landscape with multiple functional obligations contributing to fitness results in greater morphospace occupation than a landscape with just one function (Niklas 1994). Our results conceptually extend these principles to show that the effects of trade-offs may not be to just move lineages between adaptive peaks but also to increase or decrease the rate at which they traverse functional and phenotypic space.

Multifunctionality is widespread in organismal systems and our study indicates that it can elevate the exposure of these systems to trade-offs, with substantial consequences for the evolutionary dynamics of functional attributes. Nearly all organismal systems are multifunctional in some form, but the fundamental physical principles underlying organismal design provide opportunities to understand the effects of the consequential trade-offs on the evolution of those very same systems. A key goal in future work will be to test the generality of how multifunctionality impacts diversification, especially the degree to which variation among taxa in the level of multifunctionality is a major regulator of the pace of functional evolution.

Supplementary Material

Data available from the Dryad Digital Repository: https://doi.org/10.25338/B8703S.

Funding

This work was supported by a fellowship from the Achievement Rewards for College Scientists Foundation to K.A.C.; National Science Foundation grants [IOS-0444554, IOS-0924489, and DEB-1061981 to P.C.W.]; and research awards from the Center for Population Biology to K.A.C.

Acknowledgments

We thank Maxwell Rupp and Angelly Tovar for assistance with films, and Michael May for his assistance with the MuSSCRat model. Michael Turelli provided valuable feedback on the manuscript. We are grateful to the many past members of the Wainwright Lab who contributed to the videos used in this study. K.A.C. thanks Alexus Roberts and Daniel Rath for their support during this project, and Sarah Friedman for her help with tidy code.

References

Adams D.C. 2014. Quantifying and comparing phylogenetic evolutionary rates for shape and other high-dimensional phenotypic data. Syst. Biol. 63:166–177.

Adams D.C., Collyer M.L. 2018. Multivariate phylogenetic comparative methods: evaluations, comparisons, and recommendations. Syst. Biol. 67:14–31.

Adams D.C., Collyer M.L. 2019. Phylogenetic comparative methods and the evolution of multivariate phenotypes. Annu. Rev. Ecol. Evol. Syst. 50:405–425.

Adams D.C., Otárola-Castillo E. 2013. Geomorph: an r package for the collection and analysis of geometric morphometric shape data. Methods Ecol. Evol. 4:393–399.

Anker G.C. 1974. Morphology and kinetics of the head of the stickleback, *Gasterosteus aculeatus*. Trans. Zool. Soc. Lond. 32:311–416.

Beaulieu J.M., Jhwueng D.C., Boettiger C., O'Meara B.C. 2012. Modeling stabilizing selection: expanding the Ornstein–Uhlenbeck model of adaptive evolution. Evolution 66:2369–2383.

Bellwood D.R., Choat J.H. 1990. A functional analysis of grazing in parrotfishes (family Scaridae): the ecological implications. Environ. Biol. Fishes. 28:189–214.

Bemis W.E., Lauder G. V. 1986. Morphology and function of the feeding apparatus of the lungfish, *Lepidosiren paradoxa* (Dipnoi). J. Morphol. 187:81–108.

Bennett A.F., Lenski R.E. 2007. An experimental test of evolutionary trade-offs during temperature adaptation. Proc. Natl. Acad. Sci. USA 104:8649–8654.

Bishop K.L., Wainwright P.C., Holzman R.A. 2008. Anterior-to-posterior wave of buccal expansion in suction feeding fishes is critical for optimizing fluid flow velocity profile. J. R. Soc. Interface. 5:1309–16.

Camp A.L., Roberts T.J., Brainerd E.L. 2015. Swimming muscles power suction feeding in largemouth bass. Proc. Natl. Acad. Sci. USA 112:8690–8695.

Cooper N., Thomas G.H., Venditti C., Meade A., Freckleton R.P. 2016. A cautionary note on the use of Ornstein–Uhlenbeck models in macroevolutionary studies. Biol. J. Linn. Soc. 118:64–77.

Copus J.M., Gibb A.C. 2013. A forceful upper jaw facilitates picking-based prey capture: biomechanics of feeding in a butterflyfish, *Chaetodon trichrous*. Zoology 116:336–347.

Cornic A. 1987. Poissons de l'Ile Maurice. Ile Maurice: Stanley Rose Hill.

Craig M.T. 2007. Preliminary observations on the life history of the white-streaked grouper, *Epinephelus ongus*, from Okinawa, Japan. Ichthyol. Res. 54:81–84.

Dagg A.I. 1973. Gaits in mammals. Mamm. Rev. 3:135–154.

Denton J.S.S., Adams D.C. 2015. A new phylogenetic test for comparing multiple high-dimensional evolutionary rates suggests interplay of evolutionary rates and modularity in lanternfishes (Myctophiformes; Myctophidae). Evolution 69:2425–2440.

Elshoud-Oldenhave M.J.W. 1979. Prey capture in the pike-perch, *Stizostedion lucioperc*a (Teleostei, Percidae): a structural and functional analysis. Zoomorphologie 32:1–32.

Farina S.C., Knope M.L., Corn K.A., Summers A.P., Bemis W.E. 2019. Functional coupling in the evolution of suction feeding and gill ventilation of sculpins (Perciformes: Cottoidei). Integr. Comp. Biol. 59:394–409.

Feilich K.L., López-Fernández H. 2019. When does form reflect function? Acknowledging and supporting ecomorphological assumptions. Integr. Comp. Biol.:1–13.

Ferry-Graham L.A., Konow N. 2010. The intramandibular joint in Girella: a mechanism for increased force production? J. Morphol. 271:271–279.

Ferry-Graham L.A., Wainwright P.C., Bellwood D.R. 2001. Prey capture in long-jawed butterflyfishes (Chaetodontidae): the functional basis of novel feeding habits. J. Exp. Mar. Bio. Ecol. 256:167–184.

Ferry L.A., Konow N., Gibb A.C. 2012. Are kissing gourami specialized for substrate-feeding? Prey capture kinematics of *Helostoma temminckii* and other Anabantoid fishes. J. Exp. Zool. A. 317:571–579.

Friel J.P., Wainwright P.C. 1997. A model system of structural duplication: homologies of adductor mandibulae muscles in Tetraodontiform fishes. Syst. Biol. 46:441.

Futuyma D.J., Moreno G. 1988. The evolution of ecological specialization. Annu. Rev. Ecol. Syst. 19:207–233.

Gatesy S.M., Middleton K.M. 1997. Bipedalism, flight, and the evolution of theropod locomotor diversity. J. Vertebr. Paleontol. 17:308–329.

Gibb A.C., Ferry-Graham L.A. 2005. Cranial movements during suction feeding in teleost fishes: are they modified to enhance suction production? Zoology 108:141–153.

Gibb A.C., Staab K.L., Moran C., Ferry L.A. 2015. The teleost intramandibular joint: a mechanism that allows fish to obtain prey unavailable to suction feeders. Integr. Comp. Biol. 55:85–96.

Gillis G.B., Lauder G.V. 1995. Kinematics of feeding in bluegill sunfish: is there a general distinction between aquatic capture and transport behaviors? J. Exp. Biol. 198:709–720.

Gosline W.A. 1987. Jaw structures and movements in higher teleostean fishes. Jpn. J. Ichthyol. 34:21–32.

Grobecker D.B., Pietsch T.W. 1979. High-speed cinematographic evidence for ultrafast feeding in antennariid anglerfishes. Science 205:1161–1162.

Gunz P., Mitteroecker P. 2013. Semilandmarks: a method for quantifying curves and surfaces. Hystrix 24:103–109.

Hallgrímsson B., Jamniczky H., Young N.M., Rolian C., Parsons T.E., Boughner J.C., Marcucio R.S. 2009. Deciphering the palimpsest: studying the relationship between morphological integration and phenotypic covariation. Evol. Biol. 36:355–376.

Hiatt R.W., Strasburg D.W. 1960. Ecological relationships of the fish fauna on coral reefs of the marshall islands. Ecol. Monogr. 30:65–127.

Hildebrand M. 1989. The quadrupedal gaits of vertebrates. Bioscience 39:766–775.

Ho L.S.T., Ané C. 2014. Intrinsic inference difficulties for trait evolution with Ornstein–Uhlenbeck models. Methods Ecol. Evol. 5:1133–1146.

Höhna S., Landis M.J., Heath T.A., Boussau B., Lartillot N., Moore B.R., Huelsenbeck J.P., Ronquist F. 2016. RevBayes: Bayesian phylogenetic inference using graphical models and an interactive model-specification language. Syst. Biol. 65:726–736.

Holzman R.A., Collar D.C., Price S.A., Hulsey C.D., Thomson R.C., Wainwright P.C. 2012. Biomechanical trade-offs bias rates of evolution in the feeding apparatus of fishes. Proc. R. Soc. B Biol. Sci. 279:1287–1292.

Holzman R.A., Day S.W., Mehta R.S., Wainwright P.C. 2008. Jaw protrusion enhances forces exerted on prey by suction feeding fishes. J. R. Soc. Interface 5:1445–1457.

Huttegger S.M., Mitteroecker P. 2011. Invariance and meaningfulness in phenotype spaces. Evol. Biol. 38:335–351.

Jacobs C., Holzman R.A. 2018. Conserved spatio-temporal patterns of suction-feeding flows across aquatic vertebrates: a comparative flow visualization study. J. Exp. Biol.

Kendall D.G. 1984. Shape-manifolds, procrustean metrics, and complex projective spaces. Bull L. Math Soc. 16:81–121.

Koehl M.A.R. 1997. When does morphology matter? Annu. Rev. Ecol. Syst. 27:501–542.

Konow N., Bellwood D.R. 2005. Prey-capture in *Pomacanthus semicirculatus* (Teleostei, Pomacanthidae): functional implications of intramandibular joints in marine angelfishes. J. Exp. Biol. 208:1421–1433.

Konow N., Bellwood D.R., Wainwright P.C., Kerr A.M. 2008. Evolution of novel jaw joints promote trophic diversity in coral reef fishes. Biol. J. Linn. Soc. 93:545–555.

Kotrschal K. 1988. Evolutionary patterns in tropical marine reef fish feeding. J. Zool. Syst. Evol. Res. 26:51–64.
Lauder G.V. 1980a. Hydrodynamics of prey capture by teleost fishes. In: Schneck D.J., editor. Biofluid mechanics. New York, NY: Springer. p. 161–181.
Lauder G.V. 1980b. The suction feeding mechanism in sunfishes (*Lepomis* spp.): an experimental analysis. J. Exp. Biol. 88: 49–72.
Lauder G.V. 1985. Aquatic feeding in lower vertebrates. In: Hildebrand M., editor. Functional vertebrate morphology. Cambridge, MA: Harvard University Press. p. 185–229.
Liem K.F. 1978. Modulatory multiplicity in the functional repertoire of the feeding mechanism in cichlid fishes. I. Piscivores. J. Morphol. 158:323–360.
Liem K.F. 1979. Modulatory multiplicity in the feeding mechanism in cichlid fishes, as exemplified by the invertebrate pickers of Lake Tanganyika. J. Zool. 189:93–125.
Liem K.F. 1980. Adaptive significance of intra-and interspecific differences in the feeding repertoires of cichlid fishes. Am. Zool. 20:295–314.
Longo S.J., McGee M.D., Oufiero C.E., Waltzek T.B., Wainwright P.C. 2016. Body ram, not suction, is the primary axis of suction-feeding diversity in spiny-rayed fishes. J. Exp. Biol. 219:119–128.
Mackey B., Vanderploeg K., Ferry L.A. 2014. Variation in prey capture mechanics in the swordtail, *Xiphophorus helleri* in response to food type. J. Arizona-Nevada Acad. Sci. 45:59–63.
Martinez C.M., McGee M.D., Borstein S.R., Wainwright P.C. 2018. Feeding ecology underlies the evolution of cichlid jaw mobility. Evolution 72:1645–1655.
Martinez C.M., Wainwright P.C. 2019. Extending the geometric approach for studying biomechanical motions. Integr. Comp. Biol. 59:684–695.
May M.R., Moore B.R. 2019. A Bayesian approach for inferring the impact of a discrete character on rates of continuous-character evolution in the presence of background-rate variation. Syst. Biol. 69:530–544.
McGee M.D., Faircloth B.C., Borstein S.R., Zheng J., Hulsey C.D., Wainwright P.C., Alfaro M.E. 2016. Replicated divergence in cichlid radiations mirrors a major vertebrate innovation. Proc. R. Soc. B. 283:20151413.
McKaye K.R., Marsh A. 1983. Food switching by two specialized algae-scraping cichlid fishes in Lake Malawi, Africa. Oecologia 56:245–248.
Mosauer W. 1932. On the locomotion of snakes. Science 76:583–585.
Muñoz M.M., Anderson P.S.L., Patek S.N. 2017. Mechanical sensitivity and the dynamics of evolutionary rate shifts in biomechanical systems. Proc. R. Soc. B Biol. Sci. 284:20162325.
Muñoz M.M., Hu Y., Anderson P.S.L., Patek S.N. 2018. Strong biomechanical relationships bias the tempo and mode of morphological evolution. Elife 7:5607–5610.
Myers R.F. 1991. Micronesian reef fishes. Barrigada, Guam: Coral Graphics.
Niklas K.J. 1994. Morphological evolution through complex domains of fitness. Proc. Natl. Acad. Sci. USA 91:6772–6779.
Norton S.F. 1995. A functional approach to ecomorphological patterns in cottid fishes. Environ. Biol. Fishes 44:61–78.
Norton S.F., Brainerd E.L. 1993. Convergence in the feeding mechanics of ecomorphologically similar species in the Centrarchidae and Cichlidae. J. Exp. Biol. 176:11–29.
Olsen A.M., Hernandez L.P., Camp A.L., Brainerd E.L. 2019. Channel catfish use higher coordination to capture prey than to swallow. Proc. R. Soc. B Biol. Sci. 286.
Ormond R.F.G. 1980. Aggressive mimicry and other interspecific feeding associations among Red Sea coral reef predators. J. Zool. 191:247–262.
Oufiero C.E., Holzman R.A., Young F.A., Wainwright P.C. 2012. New insights from serranid fishes on the role of trade-offs in suction-feeding diversification. J. Exp. Biol. 215:3845–3855.
Paradis E., Claude J., Strimmer K. 2004. APE: analyses of phylogenetics and evolution in R language. Bioinformatics 20:289–290.
Polly P.D. 2020. Functional tradeoffs carry phenotypes across the valley of the shadow of death. Integr. Comp. Biol. 60:1268–1282.
Polly P.D., Stayton C.T., Dumont E.R., Pierce S.E., Rayfield E.J., Angielczyk K.D. 2016. Combining geometric morphometrics and finite element analysis with evolutionary modeling: towards a synthesis. J. Vertebr. Paleontol. 36:e1111225.
Purcell S.W., Bellwood D.R. 1993. A functional analysis of food procurement in two surgeonfish species, *Acanthurus nigrofuscus* and *Ctenochaetus striatus* (Acanthuridae). Environ. Biol. Fishes 37:139–159.
Rabosky D.L., Chang J., Title P.O., Cowman P.F., Sallan L., Friedman M., Kaschner K., Garilao C., Near T.J., Coll M., Alfaro M.E. 2018. An inverse latitudinal gradient in speciation rate for marine fishes. Nature 559:392–395.
Randall J.E., Allen G.R., Steene R.C. 1997. Fishes of the great barrier reef and coral sea. Honolulu, HI: University of Hawaii Press.
R Core Team. 2019. R: a language and environment for statistical computing. Vienna, Austria: R Foundation for Statistical Computing.
Revell L.J. 2012. phytools: an R package for phylogenetic comparative biology (and other things). Methods Ecol. Evol. 3:217–223.
Revell L.J. 2013. A comment on the use of stochastic character maps to estimate evolutionary rate variation in a continuously valued trait. Syst. Biol. 62:339–345.
Rohlf F.J. 2015. The tps series of software. Hystrix 26:1–4.
Rohlf F.J., Slice D. 1990. Extensions of the Procrustes method for the optimal superimposition of landmarks. Syst. Zool. 39:40.
Rupp M.F., Hulsey C.D. 2014. Influence of substrate orientation on feeding kinematics and performance of algae-grazing Lake Malawi cichlid fishes. J. Exp. Biol. 217:3057–3066.
Sanford C.P., Wainwright P.C. 2002. Use of sonomicrometry demonstrates the link between prey capture kinematics and suction pressure in largemouth bass. J. Exp. Biol. 205:3445–57.
Schaefer S.A., Lauder G.V. 1996. Testing historical hypotheses of morphological change: biomechanical decoupling in loricarioid catfishes. Evolution 50:1661–1675.
Schaeffer B., Rosen D.E. 1961. Major adaptive levels in the evolution of the actinopterygian feeding mechanism. Am. Zool. 1:187–204.
Staab K.L., Holzman R.A., Hernandez L.P., Wainwright P.C. 2012. Independently evolved upper jaw protrusion mechanisms show convergent hydrodynamic function in teleost fishes. J. Exp. Biol. 215:1456–1463.
Stayton C.T. 2015. The definition, recognition, and interpretation of convergent evolution, and two new measures for quantifying and assessing the significance of convergence. Evolution 69:2140–2153.
Stayton C.T. 2019. Performance in three shell functions predicts the phenotypic distribution of hard-shelled turtles. Evolution 73:720–734.
Tedman R.A. 1980. Comparative study of the cranial morphology of the Labrids *Choerodon venustus* and *Labroides dimidiatus* and the Scarid *Scarus fasciatus* (Pisces: Perciformes) II. Cranial myology and feeding mechanisms. Mar. Freshw. Res. 31:351–372.
Vial C., Ojeda F.P. 1990. Cephalic anatomy of the herbivorous fish *Girella laevifrons* (Osteichthyes: Kyphosidae): mechanical considerations of its trophic function. Rev. Chil. Hist. Nat. 63:247–260.
Wainwright P.C. 2007. Functional versus morphological diversity in macroevolution. Annu. Rev. Ecol. Evol. Syst. 38:381–401.
Wainwright P.C., Bellwood D.R. 2002. Ecomorphology of feeding in coral reef fishes. In: Sale P.F., editor. Coral reef fishes: dynamics and diversity in a complex ecosystem. London, UK: Academic Press. p. 33–55.
Wainwright P.C., Richard B.A. 1995. Predicting patterns of prey use from morphology of fishes. Environ. Biol. Fishes 44:97–113.
Walker J.A. 2007. A general model of functional constraints on phenotypic evolution. Am. Nat. 170:681–689.
Van Wassenbergh S., Herrel A., Adriaens D., Aerts P. 2007. No trade-off between biting and suction feeding performance in clariid catfishes. J. Exp. Biol. 210:27–36.
Westneat M.W. 1994. Transmission of force and velocity in the feeding mechanisms of labrid fishes (Teleostei, Perciformes). Zoomorphology 114:103–118.

Westneat M.W. 1995. Feeding, function, and phylogeny: Analysis of historical biomechanics in Labrid fishes using comparative methods. Syst. Biol. 44:361–383.

Westneat M.W. 2003. A biomechanical model for analysis of muscle force, power output and lower jaw motion in fishes. J. Theor. Biol. 223:269–281.

Westneat M.W. 2006. Skull biomechanics and suction feeding in fishes. In: Shadwick R.E., Lauder G. V., editors. Fish physiology series: fish biomechanics. San Diego, CA: Academic Press. p. 29–75.

Wilson D.S., Yoshimura J. 1994. On the coexistence of specialists and generalists. Am. Nat. 144:692–707.